RSC Advances

PAPER

Cite this: *RSC Adv.*, 2022, **12**, 16615

Preparation of environment-friendly solid epoxy resin with high-toughness *via* one-step banburying†

Gaobo Lou, Qing Li, Qian Jin, Qingqing Rao,* Shenyuan Fu* and Jinfeng Dai*

Solid epoxy resin is highly desired in adhesives, electronic materials and coatings due to the attractive characteristics of solvent-free, highly efficient utilization and convenient storage and transportation. However, the challenges remain in fabricating high-toughness solid epoxy resin through a facile and efficient way. Here, a high-performance environment-friendly solid epoxy resin was fabricated by employing maleic anhydride grafted ethylene-vinyl acetate copolymer (EVA-*g*-MAH) as the flexibilizer *via* one-step banburying method. The results showed that the modified epoxy resin maintained a high glass transition temperature (T_g) and thermal stability, while its impact strength, tensile toughness and flexural toughness were significantly increased compared with the neat epoxy resin. The impact strength, tensile toughness and flexural toughness of R-EM10 are improved 138%, 195% and 149%, respectively. The EVA-*g*-MAH was introduced in the epoxy matrix as a separate phase to increase toughness *via* transfer stress and dissipated energy. The attractive properties of this facile fabrication process and the high-toughness, as well as the environment-friendly performance make this solid epoxy highly promising for large-scale industrial application.

Received 26th February 2022
Accepted 12th May 2022

DOI: 10.1039/d2ra01302a

rsc.li/rsc-advances

1 Introduction

Conventional solvent-based liquid epoxy resin (EP) is widely used in adhesives, coatings, matrix composites and electrical materials due to its superior adhesive strength, favorable mechanical strength, chemical and corrosion resistance, dimensional stability and processability.[1–4] However, such liquid epoxy resin has high viscosity, so it needs to be diluted with organic solvents, such as acetone, toluene, xylene, styrene *etc.* to facilitate construction, which is extremely unfriendly to the environment by releasing harmful organic solvents and volatile substances. With the imposition of legislative restrictions on the emission of organic solvents to the atmosphere, the solvent-free solid epoxy resin has aroused much attention in recent years[5–8] due to excellent environment-friendly characteristics,[6] notable efficient utilization[9] and convenience.[8] In addition, solid epoxy can be rapidly cured at moderate temperature in several minutes,[10] thus helping to save energy on industrial production. Furthermore, solid epoxy can be stored at room temperature for a long time after being mixed with curing agent,[7] which greatly reduces the difficulty of operation technology. Based on this, solid epoxy resin is considered one of the most promising thermosetting resins with remarkable potential and application value, and can be further expanded to other fields. However, owing to the poor impact resistance and serious brittleness caused by the intrinsically high cross-linking density of epoxy resin, the main challenge still remains in fabricating novel solid epoxy resin with high toughness, as well as in liquid epoxy resin.[11–14]

For decades, many chemical and physical measures have been taken to improve the toughness of epoxy resin.[15–17] Among these, introducing a second phase modifier to the epoxy resin system, such as reactive liquid rubber,[8,18–20] thermoplastic polymers,[21–23] block copolymer[2,24] and core–shell particles[25,26] as the toughening agent is recognized as the most commonly used method. In fact, the addition of toughening agent has greatly improved the fracture toughness of epoxy resin system. Notably, the block copolymer has been widely studied as a toughening modifier because of its excellent toughening effect. Zhao *et al.*[27] synthesized a novel random epoxy-amphiphilic block copolymer (PHGEL) as a toughening agent, and the results showed that the impact strength of modified EP can be improved by 294% compared with the 13 kJ m^{-2} of neat EP after adding 4 wt% PHGEL. In addition, Kishi and his coworkers[28] developed a unique triblock copolymer PMMA-*b*-Pn-*b*-PMMA by living anionic polymerization and also applied as a toughening modifier. After adding the 20 wt% triblock co-polymers, the fracture toughness of epoxy/triblock copolymer was reached to 2530 J m^{-2}, which increased up more than twenty-fold relative compared with the neat EP. However, all the improvement for

School of Chemistry and Materials Engineering, Zhejiang A&F University, Hangzhou 311300, China. E-mail: qqrao@zafu.edu.cn; fshenyuan@sina.com; jinfengdai0601@gmail.com

† Electronic supplementary information (ESI) available. See https://doi.org/10.1039/d2ra01302a

epoxy resin toughness by introducing block copolymer was carried out in solvent-based liquid epoxy resin system. The uniform mixing of liquid epoxy resin and solid block copolymer is extremely difficult and needs to be implemented at high temperature or under the assistant of third phase, usually the organic solvent. In addition, the viscosity of epoxy resin would dramatically increase with the addition of high molecular weight polymer, and then resulting in processing difficulties and high production cost.[25,29] But these troubles can be completely avoided in solid epoxy systems. Moreover, previous reports by employing block copolymer to improve the strength of solid epoxy resin systems have never been found.

Herein, EVA-*g*-MAH was used to form the elastic particles in solid epoxy matrix by facile one-step banburying to obtain excellent ductile toughness properties. Ethylene vinyl acetate (EVA) is a copolymer of ethylene and vinyl acetate. Compared with polyethylene (PE), EVA has lower crystallinity, higher toughness and impact resistance due to the introduction of vinyl acetate into the molecular chain.[30] The characterization, mechanical property, curing behavior, dynamic mechanical properties and thermal stability of the modified epoxy resin were studied. The results of FTIR spectra and DSC demonstrated a good compatibility and uniformity between the EVA-*g*-MAH and solid epoxy resin. In addition, the solid epoxy toughened by the EVA-*g*-MAH showed the significant improvement in both fracture toughness and impact strength without decreasing tensile strength, flexural strength and thermal stability. This study provides a strategy to develop the high-toughness and environment-friendly solid epoxy resins by low-cost, facile and large-scale fabrication process.

2 Experimental

2.1 Materials

Solid epoxy resin E14 was provided by Anhui Shanfu New Material Technology Co., Ltd (PR China). Maleic anhydride grafted ethylene vinyl acetate copolymer was obtained from Huayu Plastic Materials Co., Ltd (PR China). 2-Methylimidazole (2-MI) and dicyandiamide (DCD) were purchased from Shanghai Aladdin Biochemical Technology Co., Ltd (PR China).

2.2 Preparation of EVA-*g*-MAH modified epoxy resins (R-EM)

EVA-*g*-MAH modified epoxy resin was prepared by a facile one-step banburying method. Firstly, the solid epoxy resin E14 was fully mixed with different mass contents of EVA-*g*-MAH (5, 8, 10, 12, 15 and 20 wt%) at 110 °C for 15 min in HAAKE rheometer. Then, the blends were taken out in molten state and cooled down to room temperature. Afterwards, 3 wt% DCD and 0.5 wt% 2-MI were added to the above mixtures and grinded adequately by disintegrator. The obtained powders were then transferred into the metal mold and hot pressed in the press vulcanizer at 145 °C for 25 min under 10 MPa to gain the cured EVA-*g*-MAH modified epoxy resins specimen. These samples were labeled as R-EM5, R-EM8, R-EM10, R-EM12, R-EM15 and R-EM20 corresponding to the mass contents of EVA-*g*-MAH, respectively. The specific mass composition of different resin samples was listed in Table 1. The number of prepared samples for each combination shall not be less than eight.

Table 1 The mass composition of different epoxy resin systems

Samples	E14/g	EVA-*g*-MAH/g	DCD/g	2-MI/g
E14 (neat EP)	100	0	3	0.5
R-EM5 (5 wt% EVA-*g*-MAH)	100	5	3	0.5
R-EM8 (8 wt% EVA-*g*-MAH)	100	8	3	0.5
R-EM10 (10 wt% EVA-*g*-MAH)	100	10	3	0.5
R-EM12 (12 wt% EVA-*g*-MAH)	100	12	3	0.5
R-EM15 (15 wt% EVA-*g*-MAH)	100	15	3	0.5
R-EM20 (20 wt% EVA-*g*-MAH)	100	20	3	0.5

2.3 Characterization and measurements

The microscopic morphologies of the impact and tensile fracture surface of the cured epoxy resin were observed by scanning electron microscope (SEM, FEI Inspect F50, America). A Fourier transform infrared (FT-IR) spectra (Bruker Vetex-70 IR, Germany) was employed to analyze the chemical structures of samples. The mechanical properties of cured epoxy resin were tested on the Criterion40 of MTS SANS series (China). The methods for the measurement of tensile strength and flexural strength were as per GB/T 1040.2-2006 and GB/T 9341-2000, respectively. Impact strength was determined as per GB/T 1043.1-2008 using an ZBC4000 of MTS SANS series at room temperature. The curing behavior was investigated on a differential scanning calorimetry (DSC, TA-Q2000, America) under a high-purity nitrogen atmosphere with a flowing rate of 50 mL min^{-1}. Each sample heated from 30 to 300 °C with multiple heating rates of 5, 10, 15, 20, and 25 °C min^{-1}. The blends of EVA-*g*-MAH and E14 were also tested on the DSC from 20 °C to 200 °C with the heating rate of 10 °C min^{-1}. The dynamic mechanical performance of cured epoxy resin was performed on the DMA (TA Instruments, Q800, America). All the rectangular specimens with dimensions of 30 mm × 10 mm × 2 mm were measured in a single-cantilever mode. The measurements were conducted from 25 to 250 °C with heating rate of 3 °C min^{-1} and frequency of 1 Hz. Thermal stability studies were carried out by thermogravimetric analyzer (TGA, TA-Q500, USA) under a nitrogen flow with 40 mL min^{-1}. The heating rate was 10 °C min^{-1} from 30 to 800 °C.

3 Results and discusstion

3.1 Preparation and characterization of R-EM

As shown in Fig. 1, the modified epoxy resin with high-performance was prepared by one-step banburying process based on EVA-*g*-MAH block polymer and E14. Specially, no volatile organic solvents were used during the preparation process. In addition, the maleic anhydride group introduced by EVA could reacted with the epoxy group on epoxy resin to form the cross-linking network, thus greatly enhancing the compatibility of the epoxy matrix and EVA-*g*-MAH.

Fig. 2a showed the FTIR spectra of EVA-*g*-MAH, pure epoxy resin and R-EMs. As exhibited in the results, the characteristic

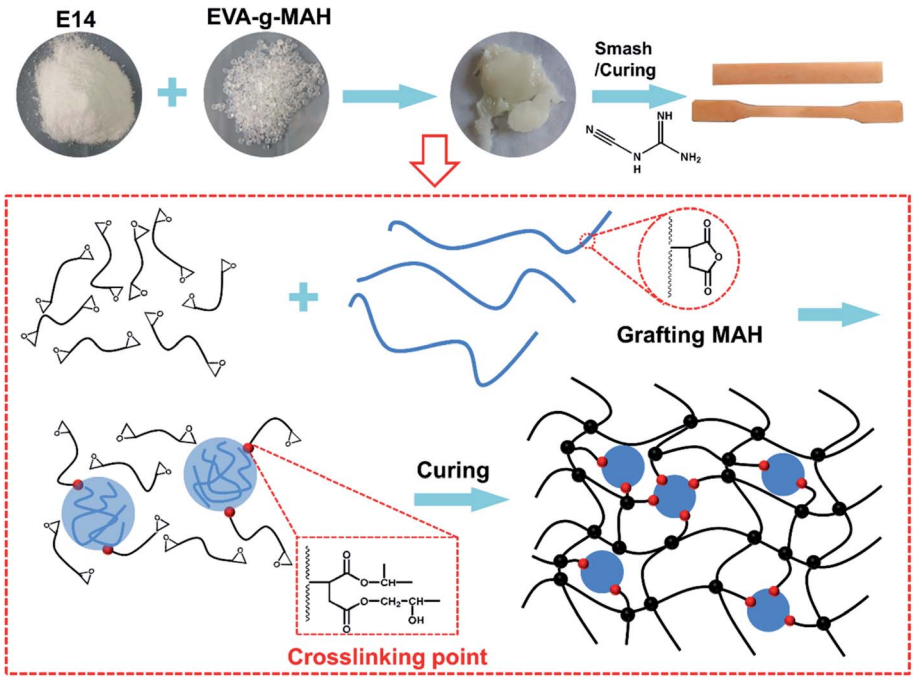

Fig. 1 Synthetic Routes of EVA-*g*-MAH modified epoxy.

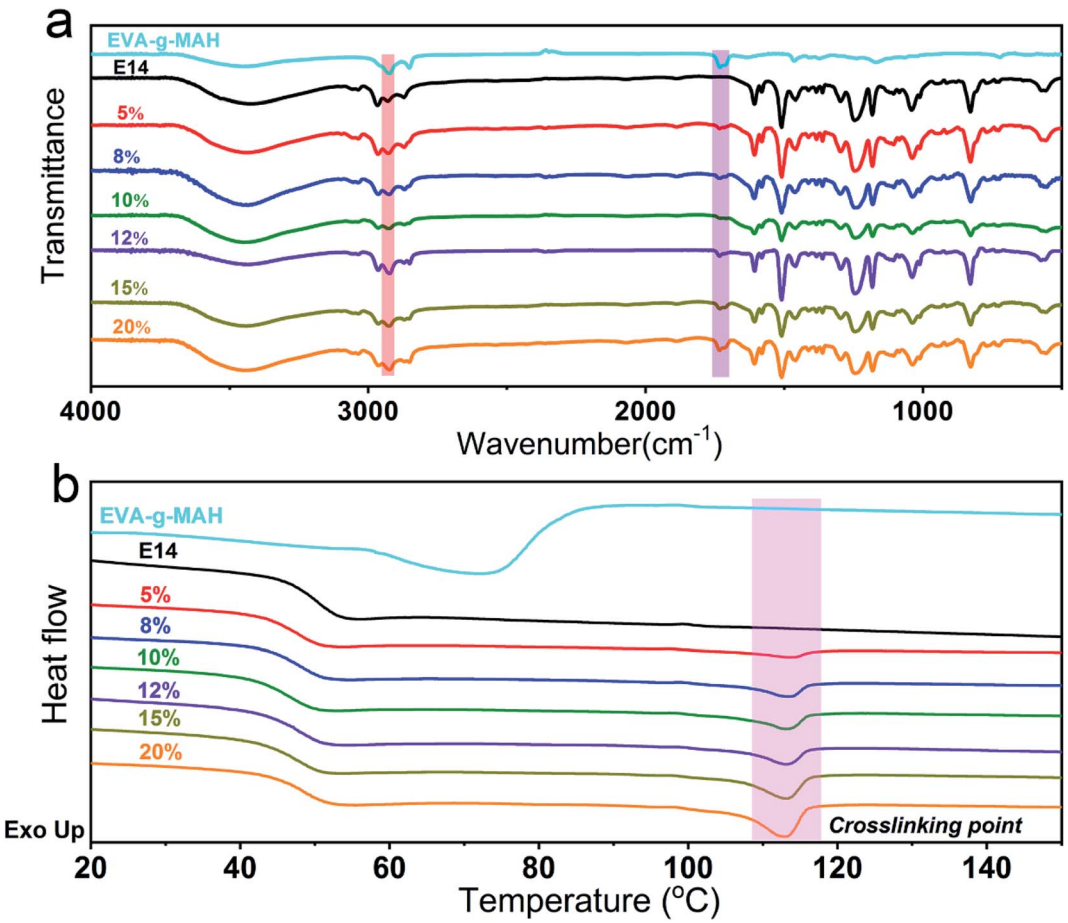

Fig. 2 (a) FTIR spectra and (b) DSC curves of EVA-*g*-MAH, E14, R-EM5, R-EM8, R-EM10, R-EM12, R-EM15 and R-EM20.

adsorption peaks observed at 2924 cm^{-1} and 1733 cm^{-1} were assigned to the stretching vibrations of C–H and C=O groups on EVA-*g*-MAH,[31–33] respectively. In addition, the intensity of adsorption peaks of C–H and C=O in the blends were gradually increased with the increase of the content of EVA-*g*-MAH content, illustrating the good compatibility between EP matrix and EVA-*g*-MAH. As shown in Fig. 2b, an endothermic peak around 114 °C was emerged after the E14 was modified by the EVA-*g*-MAH. However, no obvious endothermic peaks were observed in pure EVA-*g*-MAH and neat E14 epoxy resins. Furthermore, the endothermic enthalpy value increased with the increase of the content of EVA-*g*-MAH, indicating that a cross-linking reaction occurred between these two phases. All the results demonstrated the successful fabrication of EVA-*g*-MAH modified epoxy resin.

3.2 Mechanical performance

The impact strengths of all the cured epoxy resins with different content of EVA-*g*-MAH were shown in Fig. 3f. As presented in the results, the impact strengths of the modified epoxy resin were firstly increased with the increase of content of EVA-*g*-MAH and then gradually decreased after the amount of block polymer was greater than 12 wt%. In detail, the R-EM5, R-EM8, R-EM10, R-EM12, R-EM15 and R-EM20 were 7.0, 9.9, 12.0, 13.9, 11.0 and 8.2 kJ m^{-2}, respectively and the impact strengths of neat epoxy was only 5.1 kJ m^{-2}. Dramatically, the impact strength of R-EM12 was improved by 172% compared with neat epoxy.

Fig. 3a exhibited the un-notched impact effect of cured neat epoxy and R-EM. The efficient stress transfer and dispersion of EVA-*g*-MAH particles resulted in the remarkable improvement of epoxy resin toughness. The EVA-*g*-MAH particles were stretched by crack but still adhered to the resin due to the strong interaction between elastomer and epoxy resin. As is shown in Fig. S1†, EVA-*g*-MAH particles exhibited the strong interfacial bonding with the epoxy matrix, thus leading to most of the stress being consumed during crack growth based on the deformation and cavitation of elastomer. As shown in Fig. 3b and c, the fracture boundaries of neat epoxy resin were clear and only few plastic deformations were generated during impacting process, indicating the poor toughness of neat epoxy. In contrast, impacted R-EM10 displayed a rough and tortuous surface with significant shear deformation, showing high

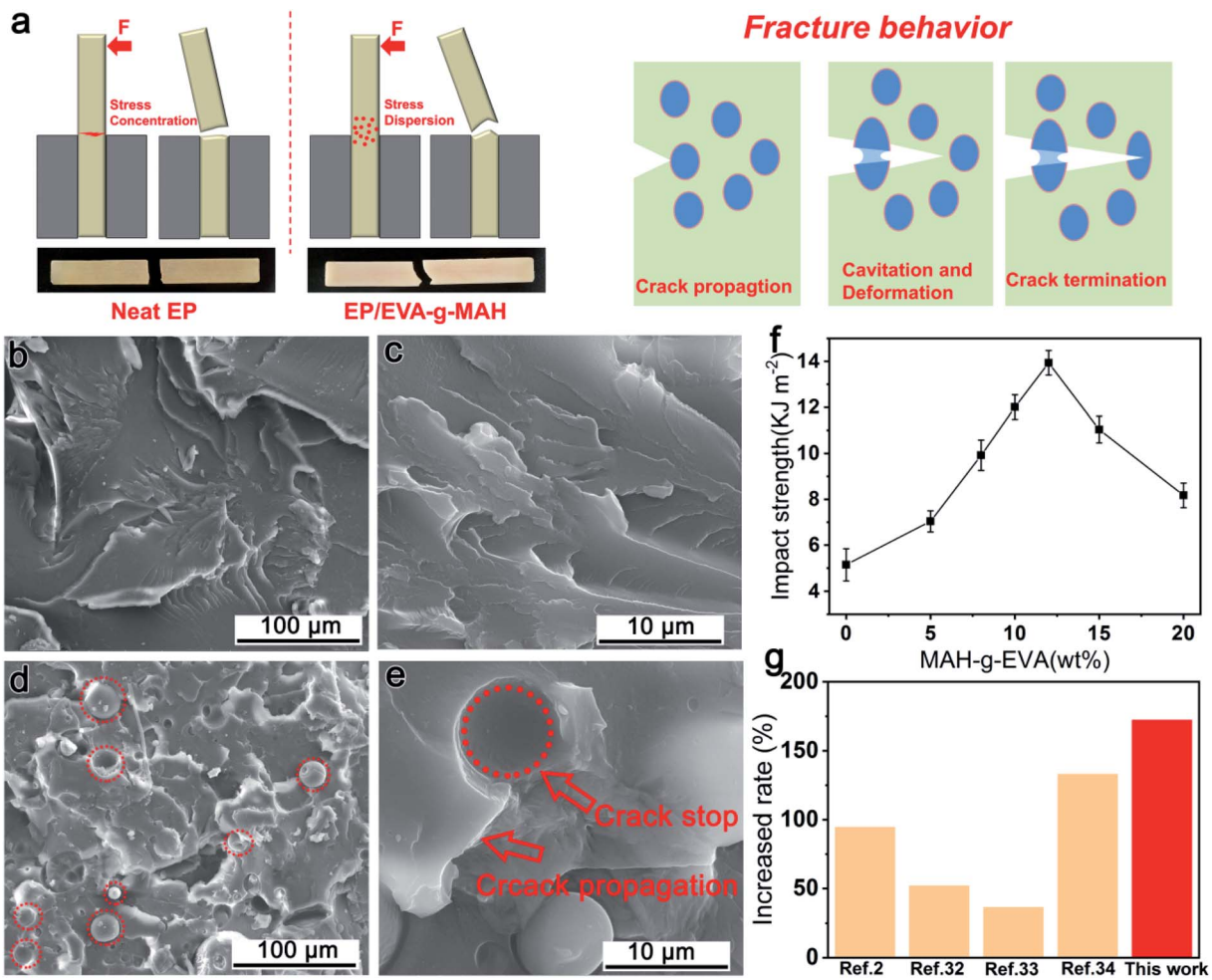

Fig. 3 (a) Schematic diagram toughening mechanism and fracture behavior. SEM micrographs of the impact fracture morphology of neat epoxy resin (b), (c) and R-EM10 (d), (e). Impact strength (f) and comparison works (g) with the effect of improving impact strength in literature.

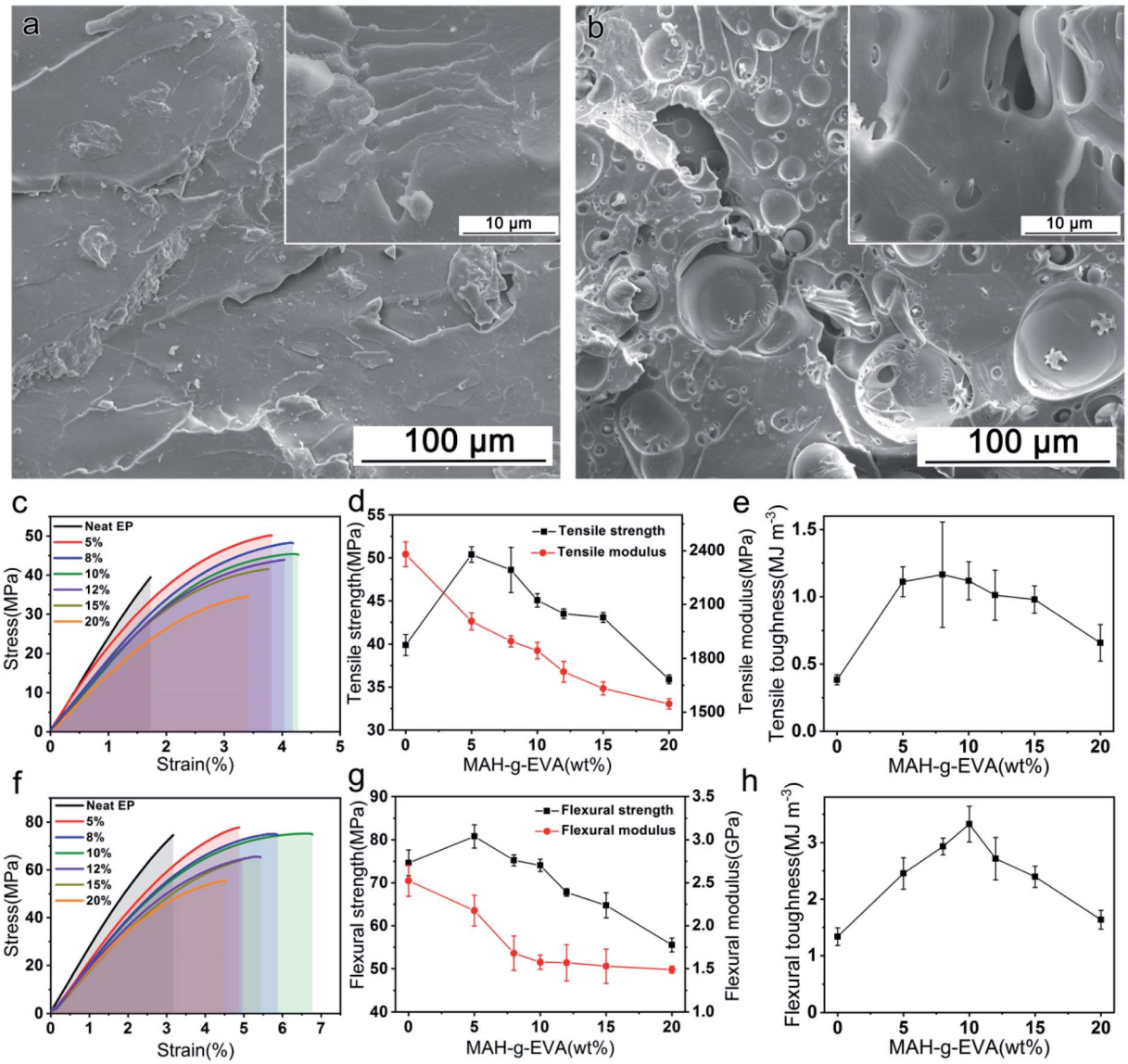

Fig. 4 SEM micrographs of the fractured surfaces of tensile specimens for neat epoxy (a) and R-EM10 (b). Stress–strain curves and mechanical properties of neat epoxy and EVA-*g*-MAH modified epoxy resins: tensile stress–strain curves (c); tensile strength and modulus (d); tensile toughness (e); flexural stress–strain curves (f); flexural strength and modulus (g) and flexural toughness (h). The toughness was calculated by the integral area enclosed by the stress–strain curves.

toughness fracture characteristic of ductile materials (Fig. 3d and e). In addition, the fracture surfaces of R-EM10 were covered with some cavity structures shown in Fig. 3e, which was speculated to be related to the cavitation of EVA-*g*-MAH particles. These cavitation phenomena could dissipate the fracture energy when cracks were generated, and then could prohibit the further growth of cracks. Hence, the fracture toughness of modified epoxy was highly improved. However, when the addition of EVA-*g*-MAH was greater than 12 wt%, the uneven mixing of EVA-*g*-MAH in epoxy matrix would result in the decrease of fracture toughness.

Besides, the increased ratios of impact strengths with some block copolymer/epoxy systems between this work and previous reports were compared.[2,34–36] As shown in Fig. 3g, the toughening effect of EVA-*g*-MAH on solid epoxy resin is better than that of some other block copolymers in liquid epoxy system, which indicates that EVA-*g*-MAH, as a cheap toughening agent, has great application prospect in solid epoxy through facile one-step banburying.

The tensile and bending properties of neat epoxy and R-EM were shown in Fig. 4 and the detailed performance parameters were listed in Table 2. As shown in Fig. 4a and b, the tensile fracture surface of R-EM10 was more twisted and rougher than that of neat epoxy resin, meanwhile, the shear deformation of the modified epoxy was serious, thus promoting the dissipation of impact energy. Fig. 4c and f presented the representative tensile and flexural stress–strain curves of epoxy resin, respectively. As shown in the results, the fracture strain was highly

Table 2 Mechanical properties of cured epoxy samples

Systems	Impact strength (kJ m^{-2})	Tensile strength (MPa)	Tensile modulus (MPa)	Tensile toughness (MJ m^{-3})	Flexural strength (MPa)	Flexural modulus (GPa)	Flexural toughness (MJ m^{-3})
Neat EP	5.1 ± 0.7	39.9 ± 1.2	2380 ± 69	0.38 ± 0.04	74.6 ± 2.9	2.52 ± 0.18	1.34 ± 0.15
R-EM5	7.0 ± 0.5	50.4 ± 0.9	2006 ± 47	1.11 ± 0.11	80.8 ± 2.7	2.17 ± 0.18	2.45 ± 0.28
R-EM8	9.9 ± 0.7	48.6 ± 2.6	1896 ± 31	1.17 ± 0.39	75.2 ± 1.3	1.68 ± 0.2	2.93 ± 0.15
R-EM10	12.0 ± 0.5	45.1 ± 0.8	1843 ± 46	1.12 ± 0.14	74.1 ± 1.4	1.58 ± 0.08	3.33 ± 0.32
R-EM12	13.9 ± 0.5	43.5 ± 0.6	1725 ± 58	1.01 ± 0.19	67.8 ± 0.9	1.57 ± 0.21	2.72 ± 0.38
R-EM15	11.0 ± 0.6	43.1 ± 0.6	1632 ± 36	0.98 ± 0.10	64.8 ± 3.0	1.53 ± 0.20	2.39 ± 0.19
R-EM20	8.2 ± 0.5	35.9 ± 0.5	1546 ± 29	0.66 ± 0.14	55.5 ± 1.6	1.49 ± 0.04	1.64 ± 0.17

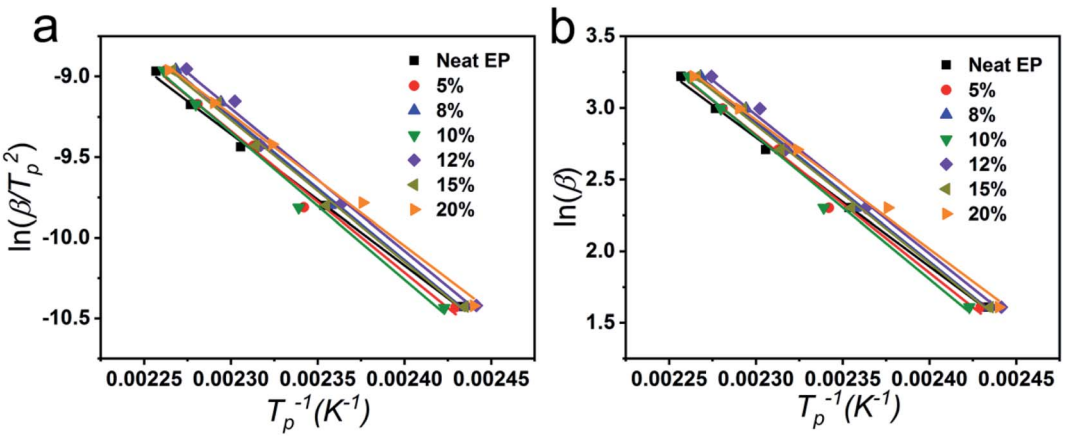

Fig. 5 Linear fitting curves of Kissinger (a) and Ozawa (b) equations of EVA-*g*-MAH modified epoxy systems.

improved after modified with EVA-*g*-MAH. The tensile and flexural strengths of R-EM were firstly increased and then reduced after the mass content of EVA-*g*-MAH was higher than 5 wt%, which was consistent with the relevant previous reports.[37–39] Besides, the toughness of all R-EM samples was enhanced compared with the neat epoxy resin (Fig. 4e and h), tensile and flexural toughness value of R-EM10 was increased by 195% and 149%, respectively, suggesting the good toughening effect of EVA-*g*-MAH.

3.3 Curing behavior

Non-isothermal curing behaviors of R-EM systems were investigated by DSC. As shown in Fig. S2,† the initial and peak temperature were improved and the curing temperature range was broadened with the increase of the heating rate, due to the increased thermal effect in per unit time.[40] The initial temperature and peak temperature during curing process were presented in Table S1.† The value of activation energy (E_a) of epoxy/EVA-*g*-MAH systems could be calculated by both of Kissinger[41] and Ozawa[42] equation during the curing of epoxy resin based on the peak temperature. Kissinger equation was expressed as follow:

$$\ln\left(\frac{\beta}{T_P^2}\right) = \ln\left(\frac{AR}{E_a}\right) - \frac{E_a}{RT_P} \quad (1)$$

where β, A, T_p, R and E_a refer to the heating rate, preexponential factor, peak temperature, gas constant (8.314 J mol^{-1} K^{-1}) and apparent activation energy, respectively.

Ozawa equation was displayed as follow:

$$\frac{d(\ln \beta)}{d(1/T_P)} = -\frac{1.052\ E_a}{R} \quad (2)$$

where β, T_p, R and E_a are the heating rate, peak temperature, gas constant (8.314 J mol^{-1} K^{-1}) and apparent activation energy, respectively.

Fig. 5a and b were the linear fitting curves based on Kissinger and Ozawa equations of epoxy/EVA-*g*-MAH systems. The E_a could be calculated by the slope of the linear fitting plot of $\ln(\beta/T_p^2)$ or $\ln(\beta)$ *versus* $1/T_p$ and the specific values of E_a were presented in Table S2.† The E_a was firstly increased and then decreased with the increase of the content of EVA-*g*-MAH. At first, the viscosity of the epoxy system was increased with the increase of EVA-*g*-MAH content, leading to the raise of activation energy. Then, the superfluous EVA-*g*-MAH aggregated in epoxy matrix with the further increase of EVA-*g*-MAH content, resulting in the phase separation and the decrease of activation energy.

Curing reaction order (n) could be calculated by crane equation as follow:

$$\frac{d(\ln \beta)}{d(1/T_P)} = -\frac{E_a}{nR} - 2T_P \quad (3)$$

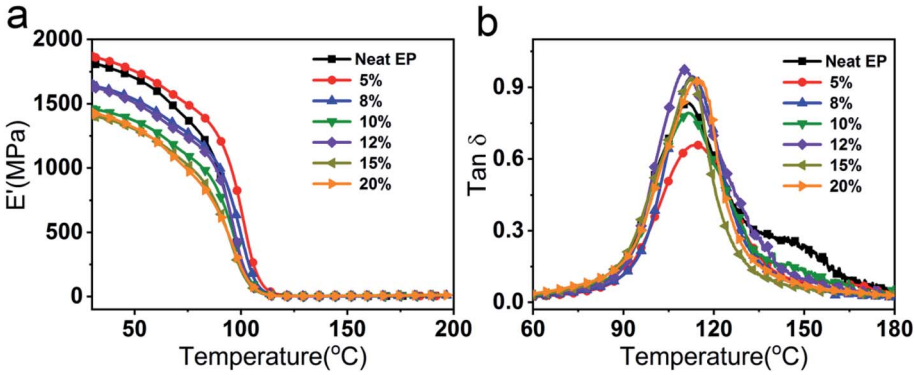

Fig. 6 Dynamic mechanical properties of cured epoxy systems: storage modulus *vs.* temperature (a) and tan δ *vs.* temperature (b).

where β, T_p, R, E_a and n are the heating rate, peak temperature, gas constant (8.314 J mol^{-1} K^{-1}), apparent activation energy and curing reaction order, respectively. The n can be obtained by plotting of $\ln(\beta) - 1/T_p$. As shown in Table S2,† the n of all solid epoxy systems was around 0.91, which suggested that the mechanism during this reaction was not be changed with the addition of EVA-*g*-MAH.

The linear fitting curves of heating rate and characteristic temperature (T_i, T_p, T_f) were shown in Fig. S3.† The theoretical gelation temperature, theoretical curing temperature and theoretical post-treatment temperature of the epoxy systems could be obtained by extrapolating the fitted equation when $\beta = 0$, the corresponding results were shown in Table S3.† According to the theoretical curing temperature, all epoxy systems with different EVA-*g*-MAH content were fully cured at temperature of 406 K to 409 K. Compared with the traditional curing process of liquid epoxy, the heat conduction efficiency during hot-pressing molding process was low, thus leading to uneven curing of solid epoxy resin. Therefore, the curing temperature in this system was appropriately increased and specified as 145 °C.

3.4 Dynamic mechanical performance

In order to explore the influence of EVA-*g*-MAH content on the thermal mechanical properties of epoxy system, the storage modulus (E') and dynamic loss (tan δ) of the cured epoxy systems were measured. As shown in Fig. 6, all the cured epoxy systems only possessed one glass transition temperature (T_g), indicating the good compatibility between EVA-*g*-MAH and epoxy matrix. In addition, as is shown in Table S4,† the T_g value of EVA-*g*-MAH modified epoxy thermosets was close to that of neat epoxy which without sacrificing T_g to improving toughness. The cross-linking density (ν_e) of the cured epoxy systems can be calculated using the classical rubber elasticity.[43,44] The corresponding equation was expressed as follows:

$$\nu_e = \frac{E'}{3RT} \quad (4)$$

where E', R and T refer to the storage modulus in rubbery plateau region at T_g + 30 °C, gas constant (8.314 J mol^{-1} K^{-1}) and absolute temperature at T_g + 30 °C, respectively.

The ν_e values were displayed in Table S4.† As exhibited in the results, the cross-linking densities of R-EM was increased compared with the neat epoxy thermosets. On the one hand, the maleic anhydride groups grafted on EVA could form some chemical crosslinking points with the epoxy groups; on the other hand, the long chain molecules could form the physical crosslinking network with the epoxy. Besides, the cross-linking density and plasticizers are the main factors affecting the T_g values of epoxy thermosets.[45] Hence, the addition of flexible molecule of EVA-*g*-MAH into the epoxy matrix would not result in the decrease of T_g.

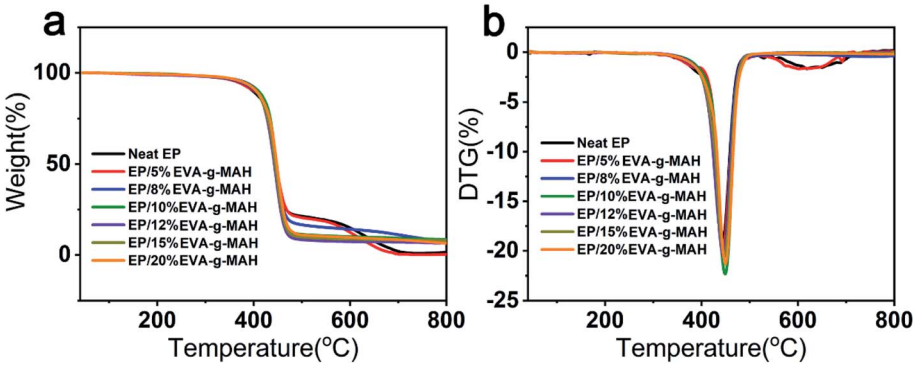

Fig. 7 TGA (a) and DTG (b) curves of cured epoxy systems.

3.5 Thermal performance

The excellent thermal stability is an outstanding performance for epoxy resin system.[46] Fig. 7a and b were the TGA and DTG curves of neat epoxy and R-EMs. The corresponding parameters, including the decomposition temperatures at 5 wt% mass loss ($T_{5\%}$), the maximum degradation temperature (T_{max}), and the char yield at 800 °C were presented in Table S5.† As shown in the results, the $T_{5\%}$, T_{max} and the char yield at 800 °C of the modified epoxy resin were higher than that of the neat epoxy resin when the mass content of EVA-*g*-MAH was more than 5 wt%, suggesting that a certain amount of EVA-*g*-MAH can improve the thermal stability of the epoxy resin. The EVA-*g*-MAH acting as the end-capping advanced the protection and enhancement effect of cross-linked network of epoxy resin.[8] When the content of EVA-*g*-MAH was 10 wt%, the thermal stability of epoxy resin was the highest. Specifically, the $T_{5\%}$, T_{max} and the char yield at 800 °C of neat epoxy resin increased from 368.1 °C, 444.4 °C and 1.5% to 380.7 °C, 449.1 °C and 8.5%, respectively.

4 Conclusion

In this study, we synthesized a high-performance solvent free solid epoxy resin by using EVA-*g*-MAH as a toughening agent through a one-step processing method. The EVA-*g*-MAH showed an excellent toughening effect on epoxy thermoset *via* transfer stress and dissipated energy, meanwhile, the EVA-*g*-MAH modified epoxy resin maintained high glass transition temperature. In addition, the impact strength, tensile toughness and flexural toughness of R-EM10 were improved 138%, 195% and 149%, respectively. Moreover, the activation energy of EVA-*g*-MAH modified epoxy resins during the curing process was firstly increased and then decreased because of the viscosity and phase separation of the system. Furthermore, the thermostability of modified epoxy resin was highly enhanced. The findings in this work provides a facile pathway to prepare a high-performance solid epoxy resin that has tremendous valuable for industrial application.

Author contributions

All authors have given approval to the final version of the manuscript.

Conflicts of interest

The authors declare no competing financial interest.

Acknowledgements

This work was financially supported by the "Top soldiers" and "Leading geese" projects of Zhejiang Provincial Department of Science and Technology (2022C03128), the National Natural Science Foundation of China (No. 51903222), the National Natural Science Foundation of Zhejiang Province (No. LY21E030001).

References

1 X. Xiong, L. Zhou, R. Ren, X. Ma and P. Chen, *Polymer*, 2018, **140**, 326–333.
2 L. Tao, Z. Sun, W. Min, H. Ou, L. Qi and M. Yu, *RSC Adv.*, 2020, **10**, 1603–1612.
3 J. Jung and H. A. Sodano, *Polymer*, 2020, 122438.
4 K. Xu, C. Li, C. Wang, Y. Jiang, Y. Liu and H. Xie, *J. Therm. Anal. Calorim.*, 2019, **137**, 1189–1198.
5 D. Shikha, P. Kamani and M. Shukla, *Prog. Org. Coat.*, 2003, **47**, 87–94.
6 J. Xu, J. Yang, X. Liu, H. Wang, J. Zhang and S. Fu, *R. Soc. Open Sci*, 2018, **5**, 180566.
7 T. Vidil, F. Tournilhac, S. Musso, A. Robisson and L. Leibler, *Prog. Polym. Sci.*, 2016, **62**, 126–179.
8 J. Yang, X. He, H. Wang, X. Liu, P. Lin, S. Yang and S. Fu, *J. Appl. Polym. Sci.*, 2020, **137**, 48596.
9 Z. Khanam, V. Singh and M. G. H. Zaidi, *Polym. Adv. Technol.*, 2018, **29**, 2457–2466.
10 A. Keller, K. Masania, A. Taylor and C. Dransfeld, *J. Mater. Sci.*, 2016, **51**, 236–251.
11 R. Auvergne, S. Caillol, G. David, B. Boutevin and J.-P. Pascault, *Chem. Rev.*, 2014, **114**, 1082–1115.
12 H. Yin, H. Jin, C. Wang, Y. Sun, Z. Yuan, H. Xie, Z. Wang and R. Cheng, *J. Therm. Anal. Calorim.*, 2014, **115**, 1073–1080.
13 M. Lee, W. Kwon, D. Kwon, E. Lee and E. Jeong, *J. Ind. Eng. Chem.*, 2019, **77**, 461–469.
14 S. Cai, Y. Li, H.-Y. Liu and Y.-W. Mai, *Compos. Sci. Technol.*, 2019, **181**, 107673.
15 J. J. Chruściel and E. Leśniak, *Prog. Polym. Sci.*, 2015, **41**, 67–121.
16 W.-C. Lai and R.-Y. Hsia, *Polymer*, 2018, **147**, 74–80.
17 J. S. Lee, N. Y. Ko, N. H. Kwak, W. B. Ying and B. Lee, *J. Appl. Polym. Sci.*, 2019, **136**, 48178.
18 P. Vijayan, D. Puglia, P. Vijayan, J. M. Kenny and S. Thomas, *Mater. Technol.*, 2017, **32**, 171–177.
19 R. Konnola, J. Parameswaranpillai and K. Joseph, *Polym. Compos.*, 2016, **37**, 2109–2120.
20 X. Song and S. Xu, *J. Therm. Anal. Calorim.*, 2016, **123**, 319–327.
21 R. Brooker, A. Kinloch and A. Taylor, *J. Adhes.*, 2010, **86**, 726–741.
22 N. Mahnam, M. H. Beheshty, M. Barmar and M. Shervin, *High Perform. Polym.*, 2013, **25**, 705–713.
23 D. Puglia, M. A. S. Al-Maadeed, J. M. Kenny and S. Thomas, *Mater. Sci. Eng., R*, 2017, **116**, 1–29.
24 Z. J. Thompson, M. A. Hillmyer, J. Liu, H.-J. Sue, M. Dettloff and F. S. Bates, *Macromolecules*, 2009, **42**, 2333–2335.
25 J. Wang, Z. Xue, Y. Li, G. Li, Y. Wang, W.-H. Zhong and X. Yang, *Polymer*, 2018, **140**, 39–46.
26 S. Liu, X. Fan and C. He, *Compos. Sci. Technol.*, 2016, **125**, 132–140.
27 F. Zhao, X. Fei, W. Wei, W. Ye, J. Luo, Y. Chen, Y. Zhu and X. Liu, *J. Appl. Polym. Sci.*, 2017, **134**, 44863.
28 H. Kishi, Y. Kunimitsu, J. Imade, S. Oshita, Y. Morishita and M. Asada, *Polymer*, 2011, **52**, 760–768.

29 G. Di Pasquale, O. Motto, A. Rocca, J. Carter, P. McGrail and D. Acierno, *Polymer*, 1997, **38**, 4345–4348.
30 A. Zubkiewicz, A. Szymczyk, S. Paszkiewicz, R. Jędrzejewski, E. Piesowicz and J. Siemiński, *J. Appl. Polym. Sci.*, 2020, 49135.
31 T. Wang, D. Liu and C. Xiong, *J. Mater. Sci.*, 2007, **42**, 3398.
32 Q.-V. Bach, C. M. Vu, H. T. Vu, T. Hoang, T. V. Dieu and D. D. Nguyen, *Polym. J*, 2019, 1–13.
33 M. D. Shokrian, K. Shelesh-Nezhad and R. Najjar, *Polymer*, 2019, **168**, 104–115.
34 R. He, X. Zhan, Q. Zhang, G. Zhang and F. Chen, *Polymer*, 2016, **92**, 222–230.
35 H. Li, Z. Liu, J. Gu, D. Wang, C. Qu, X. Bai and Y. Qiao, *Nanocomposites*, 2019, **5**, 28–35.
36 A. Mirmohseni and S. Zavareh, *J. Polym. Res.*, 2010, **17**, 191–201.
37 M. Goyat, S. Rana, S. Halder and P. Ghosh, *Ultrason. Sonochem.*, 2018, **40**, 861–873.
38 L. Kregl, G. M. Wallner, R. W. Lang and G. Mayrhofer, *J. Appl. Polym. Sci.*, 2017, **134**, 45348.
39 J. Song, C. Chen, S. Zhu, M. Zhu, J. Dai, U. Ray, Y. Li, Y. Kuang, Y. Li and N. Quispe, *Nature*, 2018, **554**, 224–228.
40 D. A. Lakho, D. Yao, K. Cho, M. Ishaq and Y. Wang, *Polym.-Plast. Technol. Eng.*, 2017, **56**, 161–170.
41 H. E. Kissinger, *J. Res. Natl. Bur. Stand.*, 1956, **57**, 217.
42 T. Ozawa, *Bull. Chem. Soc. Jpn.*, 1965, **38**, 1881–1886.
43 W. D. Cook, T. L. Schiller, F. Chen, C. Moorhoff, S. H. Thang, C. N. Bowman and T. F. Scott, *Macromolecules*, 2012, **45**, 9734–9741.
44 X. Pan and D. C. Webster, *Macromol. Rapid Commun.*, 2011, **32**, 1324–1330.
45 S. Chen, B. Chen, J. Fan and J. Feng, *ACS Sustainable Chem. Eng.*, 2015, **3**, 2077–2083.
46 S. Li, Q. Lin, H. Zhu, H. Hou, Y. Li, Q. Wu and C. Cui, *Polym. Adv. Technol.*, 2016, **27**, 898–904.